

# Mitigation of Eutrophication and Hypoxia through Oyster Aquaculture: An Ecosystem Model Evaluation off the Pearl River Estuary

Liuqian Yu and Jianping Gan\*



Cite This: *Environ. Sci. Technol.* 2021, 55, 5506–5514



Read Online

ACCESS |



Metrics & More



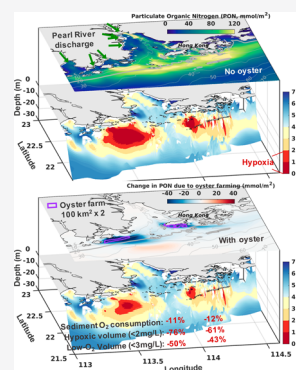
Article Recommendations



Supporting Information

**ABSTRACT:** Shellfish aquaculture has been proposed to abate eutrophication because it can remove nutrients via shellfish filter-feeding. Using a three-dimensional physical-biogeochemical model, we investigate how effective oyster aquaculture can alleviate eutrophication-driven hypoxia off the Pearl River Estuary. Results show that oysters reduce sediment oxygen consumption and thus hypoxia, by reducing both particulate organic matter directly and regenerated nutrients that support new production of organic matter. The hypoxia reduction is largest when oysters are farmed within the upper water of the low-oxygen zone, and the reduction increases with increasing oyster density although oyster growth becomes slower due to food limitation. When oysters are farmed upstream of the hypoxic zone, the farming-induced hypoxia reduction is small and it declines with increasing oyster density because the nutrients released from the farm can increase downstream organic matter production. An oyster farming area of 10 to 200 km<sup>2</sup> yields a hypoxic volume reduction of 10% to 78%, equaling the impact of reducing 10% to 60% of river nutrient input. Our results demonstrate that oyster aquaculture can mitigate eutrophication and hypoxia, but its effectiveness depends on the farming location, areal size, and oyster density, and optimal designs must take into account the circulation and biogeochemical characteristics of the specific ecosystem.

**KEYWORDS:** Shellfish aquaculture, Nutrient removal, Hypoxia abatement, Physical-biogeochemical model, Oyster model



## INTRODUCTION

Excessive anthropogenic nutrient loading has contributed to the global expansion of coastal eutrophication and hypoxic zones (dissolved oxygen < 2 mg/L) over recent decades.<sup>1,2</sup> Recognizing the detrimental effects of eutrophication and hypoxia on aquatic ecosystems,<sup>3</sup> numerous resources have been dedicated to reducing anthropogenic nutrient loads.<sup>4</sup> Nevertheless, coastal eutrophication and hypoxia are still pervasive and growing worldwide, partly due to other stressors working in parallel (e.g., warming, increasing runoff)<sup>5</sup> and the legacy of earlier eutrophication (e.g., sediment phosphorus release).<sup>6,7</sup> As a result, additional nutrient abatement strategies have been called on to complement conventional land-based measures (i.e., those measures that aim to eliminate or reduce emissions at the source of the pollution from land).<sup>4</sup>

One complementary measure that has gained increasing attention is shellfish aquaculture and/or restoration.<sup>8–15</sup> The filter-feeding activities of shellfish naturally remove the nutrients contained in plankton and particulate organic matter, often referred to as “nutrient bioextraction”.<sup>9,16</sup> In the case of shellfish aquaculture, the nutrients incorporated in shellfish biomass are permanently removed from the aquatic system when the shellfish are harvested. This nutrient bioextraction differs from the land-based abatement strategies in that it removes nutrients that have already reached the aquatic environment. Bioextraction is especially valuable when land-

based strategies to further reduce nutrient emissions, particularly from diffuse nonpoint sources (e.g., runoff and atmospheric deposition), become technically infeasible or cost-inefficient.<sup>12</sup> Furthermore, in aquatic systems where sediment nutrient release greatly contributes to total nutrient loading (e.g., Baltic Sea),<sup>17,18</sup> nutrient bioextraction through shellfish in the affected ecosystem might be the only natural solution available as the sediment nutrient release cannot be addressed by land-based measures.<sup>19</sup> It is also worth noting that cultivation of shellfish generally has a lower environmental impact than other forms of aquaculture because it does not require any artificial feed inputs.<sup>20</sup>

Currently, using shellfish aquaculture for abating eutrophication has been evaluated in a variety of estuarine and coastal systems, mostly located in Europe and the United States (see Bricker<sup>10</sup> and references therein). These studies found that shellfish aquaculture can be more cost-efficient than the conventional nonpoint source management strategies,<sup>15,21,22</sup>

**Received:** October 1, 2020

**Revised:** January 11, 2021

**Accepted:** March 11, 2021

**Published:** March 24, 2021



and the promising evaluations have spurred the policy initiatives of expanding shellfish aquaculture in many regions. For example, mussel farming is proposed as an internal measure to regulate the nutrient levels in the Baltic Sea,<sup>11,12,23,24</sup> and oyster aquaculture and restoration have been proposed for the Chesapeake Bay,<sup>13,25</sup> Long Island Sound,<sup>10</sup> and Rhode Island.<sup>26</sup> However, previous studies on the prospect of large-scale shellfish farming often rely on upscaling the measured or model-simulated nitrogen removal results at local scales (i.e., farm-scale) to obtain system-wide removal estimates.<sup>8,15,22,24</sup> The upscaling might overlook the complex, nonlinear interactions between shellfish filtration and ecosystem responses whose effects can be magnified when expanding the areal size of the shellfish farm or increasing the cultivation density. Furthermore, bottom water hypoxia is recognized as one of the most damaging consequences of eutrophication, but the potential of large-scale shellfish aquaculture to alleviate hypoxia remains understudied.

This study aims to provide quantitative understanding and implications for using shellfish aquaculture to abate eutrophication and hypoxia in estuarine and coastal ecosystems. To this end, we incorporate an oyster module into a three-dimensional (3D) coupled physical-biogeochemical model to allow simulation of the interactive hydrodynamics and biogeochemical processes associated with nutrient cycling, oxygen dynamics, and shellfish filter-feeding activities. Using the model, we quantify how effective different oyster aquaculture strategies (e.g., farming location, areal size, and cultivation density) can remove nutrients and mitigate hypoxia in a large eutrophic estuary, the Pearl River Estuary, under dynamic biophysical conditions.

## MATERIALS AND METHODS

### 2.1. Study Region.

The Pearl River Estuary (PRE) and its adjacent shelf waters off the northern South China Sea represent an estuarine marine system that is under intensive anthropogenic stressors. One major stressor is the excess nutrients delivered by the Pearl River, the second-largest river in China in terms of freshwater discharge ( $3.26 \times 10^{11} \text{ m}^3 \text{ yr}^{-1}$ ).<sup>27</sup> During the wet season (April to September), when nearly 80% of the Pearl River discharge occurs and the southwesterly wind prevails, the strong seaward buoyant surface flow converges with the wind-driven along-shelf current in the coastal transition zone off the PRE (Figure 1). This convergence creates a stable water column with long residence time that favors accumulating autochthonous organic matter (OM) from phytoplankton blooms and the allochthonous OM supplied by river runoff. The accumulation of OM ultimately promotes hypoxia development in the coastal transition zone (Figure 1).<sup>28,29</sup> The PRE has a long history of and huge market demand for oyster aquaculture. The oyster farming area within the PRE is about  $140 \text{ km}^2$ , accounting for approximately 10% of the total oyster aquaculture area in China (China Fishery Statistical Yearbook, 2019).<sup>30</sup> This scale of farming is significant considering that China supplied about 86% of global oyster aquaculture by weight in 2016.<sup>31</sup> These oyster farms are mostly located in the estuary and nearshore regions (SI Figure S1). Their effects on nutrient and oxygen dynamics are worth future investigation, but will not be addressed in this work. Instead, we investigate the effectiveness of alternative farming strategies in the coastal transition zone off the PRE for nutrient removal and hypoxia mitigation.

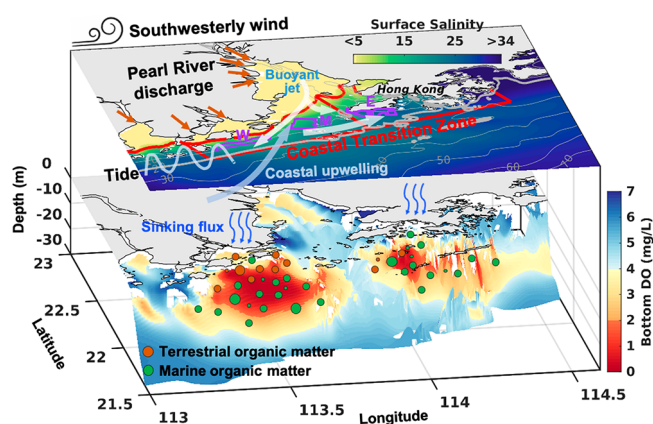


**Figure 1.** Overview of characteristic forcing, hydrodynamics, and bottom water hypoxia distribution off the Pearl River Estuary. The three-dimensional view shows the model-simulated surface salinity on the top and bottom dissolved oxygen (DO) concentration superimposed onto the topography. The model domain extends to 80 m depth, but only the top 30 m is shown in the bottom colormap. In the surface colormap, the solid red curves represent the simulated bottom salinity contour of 10, which with the solid red straight lines, denote the western and eastern coastal transition zone. The three magenta rectangles from west to east denote the location of the  $100\text{-km}^2$  oyster farm in the model experiment “W”, “M”, and “E”, respectively.

### 2.2. Coupled Physical-Biogeochemical Model.

The physical component of our coupled model is a 3D high-resolution (horizontal resolution of 0.1 to 1 km) configuration of the Regional Ocean Modeling System (ROMS)<sup>32</sup> for the PRE and its adjacent shelf.<sup>33</sup> The biogeochemical component is based on the pelagic nitrogen cycle model of Fennel<sup>34</sup> that was expanded to include oxygen,<sup>35</sup> phosphate,<sup>36</sup> and terrestrial organic matter.<sup>29</sup> Detailed model setup is presented in SI (Text S1) and extensive model validation can be found in Li<sup>28</sup> and Yu.<sup>29</sup>

For this study, we further expanded the biogeochemical model to incorporate the filter-feeding activities of oysters (Figure 2). The construction of the oyster module largely follows Cerco and Noel<sup>13,37</sup> but was adapted to focus on how oyster filtration affects the nutrient cycle and oxygen-related processes instead of on how filtration changes oyster biomass. Therefore, rather than explicitly including a state variable to represent oysters or simulating the temporal change in oyster biomass, the tissue biomass of each oyster was fixed at 1 g dry weight (DW) during our 45-day simulation period. This is roughly the average weight (0.60–1.27 g DW) of the medium-size *Crassostrea angulata*, one of the major oyster culture species in southern China, during summer.<sup>38</sup> We present the essential oyster-related parametrizations added to the model here, while the full set of equations, parameter values, and references are available in Tables S1–S3 of SI.

The main oyster processes parametrized in the model are as shown below (Figure 2).

**Filtration.** The oyster filtrates particulate organic matter (POM), including phytoplankton, zooplankton, small and large detritus, and terrestrial particulate organic matter ( $\text{POM}_{\text{terr}}$ ). The rate of POM filtrated by oyster is estimated as the product of filtration rate (i.e., the volume of water filtered per unit of time by oyster) and the POM concentration of the filtered water. The filtration rate ( $FR$ ,  $\text{m}^3/(\text{g DW})/\text{day}$ ) is based on the temperature-dependent standardized filtration rate ( $FR_o(T)$ ,  $\text{m}^3/(\text{g DW})/\text{day}$ ) of the *Crassostrea angulata*

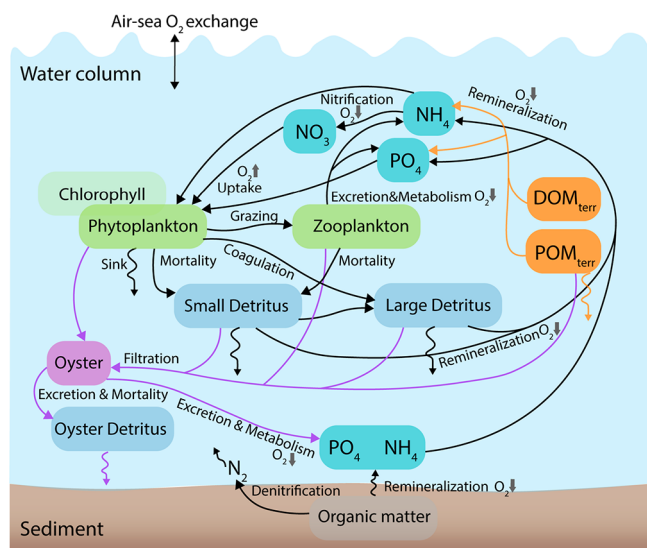


**Figure 2.** Schematic of the biogeochemical model representing the ecosystem processes and pathways. Biogeochemical processes that produce and consume oxygen are indicated with up and down thick black arrows, respectively. Processes and pathways related to the oyster are in purple.

measured at an oyster farm near the PRE.<sup>38</sup> Following Cerco and Noel,<sup>37</sup> we multiplied  $FR_o(T)$  by two environmental limitation functions, scaled between 0 and 1, to account for the effects of salinity and dissolved oxygen concentration on filtration

$$FR = FR_o(T) \cdot f(S) \cdot f(O_2) \quad (1)$$

where  $f(S)$  is based on lab experiments of oysters collected from local farms in the PRE<sup>39</sup> and  $f(O_2)$  is adopted from the empirical function in Cerco and Noel.<sup>37</sup>

**Ingestion and assimilation.** The oyster expels the filtered POM that exceeds its maximum ingestion capacity as pseudofeces.<sup>37</sup> Furthermore, the oyster assimilates only a fraction of the ingested food while the unassimilated fraction is excreted as feces. Both pseudofeces and feces enter the pool of oyster detritus.

**Basal metabolism and active respiration.** Oyster basal metabolism (or passive respiration) is parametrized as a constant fraction of oyster biomass with temperature dependency, whereas active respiration due to oyster acquiring and assimilating food is formulated as a constant fraction of the assimilated food. Both processes consume oxygen.

**Excretion.** Oyster basal metabolism and feeding excrete ammonium ( $NH_4$ ) and phosphate ( $PO_4$ ) that we assume are in Redfield stoichiometry.

**Mortality.** Mortality of the oyster from all sources other than harvest is parametrized as a constant first-order term, which acts as a source of oyster detritus.

**Sinking.** Vertical sinking of the oyster detritus (25 m/day) is set to be much faster than the sinking of other types of detritus (1 and 10 m/day for small and large detritus, respectively).

**Remineralization.** Remineralization of the oyster detritus occurs in the water column and at the water-sediment interface, analogous to other detrital POM.

Suspended cultivation is commonly adopted in oyster aquaculture, where oysters are held in floating cages or bags or attached to long lines in the water column above the seabed. To mimic the suspended aquaculture, we parametrized the

depth of the oyster farms to be approximately 1.2 m below the surface water. Filtration and feeding activities of oysters are limited to the predefined farming area because the cultured oysters could not actively or passively drift; however, the expelled pseudofeces, feces, and excreted nutrients from oysters are free to flow with the ocean current. Considering that the oyster farming unit is relatively small and that the wind-driven shelf current is generally strong off the PRE, we neglect the modulating effect of oyster farms on the flow fields.

The coupled physical-biogeochemical model uses realistic topography and is forced by the typical summer river forcing, the prevailing southwesterly monsoon wind, and tides. The detailed implementations of the forcing and justifications are provided in the SI (Text S1).

**2.3. Model Experiments.** We conducted a model experiment that had no oyster aquaculture, which we based on the original model without oyster-associated processes and referred to as the “No\_oyster” case. Then we conducted a series of oyster model simulations based on the extended model with oyster dynamics. The oyster model simulations had setups identical to the No\_oyster case except that we ran the model under different aquaculture scenarios to evaluate the effects of oyster aquaculture location, cultivation density, and farm size.

Specifically, to evaluate the impact of oyster aquaculture location, we conducted three simulations with an oyster farm in the western (denoted as Case “W”), middle (“M”), and eastern (“E”) part of the coastal transition zone, respectively (Figure 1). We defined the farm areal size to be 100 km<sup>2</sup> with an oyster density of 200 oysters/m<sup>2</sup> in each of the three cases. We conducted one additional experiment called “WE” where an aquaculture area of 200 km<sup>2</sup>, combining the farms in the W and E cases, was implemented. For WE, the oyster density was kept at 200 oysters/m<sup>2</sup>.

To evaluate the impact of oyster cultivation density, we conducted four simulations whose setups were identical to the W case, but we adjusted the oyster density from 200 to 50 (Case “Wd50”), 100 (“Wd100”), 300 (“Wd300”), or 400 oysters/m<sup>2</sup> (“Wd400”). The chosen density levels are within the range of real densities adopted in commercial oyster farms.<sup>38,40</sup> Next, to evaluate the impact of oyster farming areal size, we conducted four additional simulations that had the same setup as the W case, but we shrunk or expanded the farming area from 100 km<sup>2</sup> to 10 (Case “Wa10”), 25 (“Wa25”), 50 (“Wa50”), or 200 km<sup>2</sup> (“Wa200”).

Lastly, to compare the effectiveness of hypoxia reduction by oyster aquaculture to the riverine nutrient reduction approach, we conducted a series of river nutrient reduction experiments. These experiments used the same model setup as the No\_oyster case except that we decreased concentrations of river nutrients (i.e.,  $NO_3$ ,  $NH_4$ , and  $PO_4$ ) by 10%, 20%, 30%, 40%, 50%, or 60%. We refer to the experiments as ‘-x%RivNtr’ where  $x$  denotes the percentage nutrient reduction.

All model simulations were run for 45 days, during which the model-simulated biogeochemical fields reached quasi-steady states after about 30 days.<sup>29</sup> Model results for the entire PRE and its adjacent shelf were outputted daily, and our analyses used the results averaged over a full spring-neap tidal cycle from Day 38 (during neap tide) to Day 45 (during spring tide), which allows us to focus on the subtidal net effect. The analyses primarily focus on the coastal transition zone, which covers the area where hypoxia frequently occurs<sup>28</sup> and is bounded by the model-simulated bottom salinity contour of 10

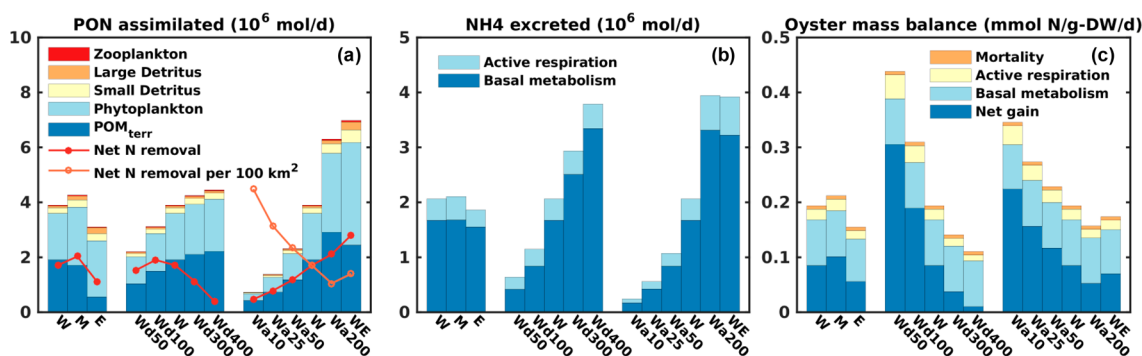


**Figure 3.** Domain integrated rate of (a) oyster assimilated particulate organic nitrogen (PON), (b) oyster excreted  $\text{NH}_4$ , and (c) oyster related terms normalized by total dry weights of oysters for different farming cases. In panel a, the dotted red lines denote the net N removal (i.e., the difference between assimilated PON and excreted  $\text{NH}_4$  and oyster mortality), and the dotted orange lines denote the normalized net N removal per  $100 \text{ km}^2$  of the farming area.

in the north and a straight line largely following the 30 m depth contour in the south (Figure 1). The transition zone is further divided into western (upstream) and eastern (downstream) zones where two hypoxia hotspots locate.<sup>28</sup>

## RESULTS AND DISCUSSION

**3.1. Model Validation.** The model simulated hydrodynamics were substantially validated in Liu and Gan,<sup>33</sup> while the simulated biogeochemical fields from the model without oyster-associated dynamics were rigorously validated by Yu<sup>29</sup> and Li.<sup>28</sup> All validations showed that the model realistically captures the physical-biogeochemical responses to river discharge and the wind-driven shelf current. The model also reproduces the observed bottom water hypoxia, which is largely distributed within the coastal transition zone (Figure 1). For this study, we validate the simulated oyster-related processes newly added to the model.

First, we examine whether the model could produce the optimal locations for oyster aquaculture. To this end, we calculated a feasibility index defined as the product of the oyster filtration rate (affected by temperature, salinity, and oxygen) and the particulate organic nitrogen (PON) concentration (to represent food availability). The higher the index, the more suited the area is for oyster aquaculture. The spatial distribution of the feasibility of farming locations is in the SI Figure S1. The existing oyster farms are distributed in areas of high model-simulated aquaculture feasibility, proving that the model can realistically represent the suitable environmental and food conditions for oyster farming. The coastal transition zone also has very high farming feasibility, largely owing to the convergence-induced accumulation of organic matter, and thus serves as suitable locations for future expansion of oyster aquaculture in the region.

Next, we assess whether the model simulated key oyster-related process rates agree with available observations. The comparison of model simulations and data is summarized in Table S4 of the SI in which the model estimates are based on Case W and spatially averaged over the entire farming area. The comparison indicates that the simulated oyster filtration rate (on average  $0.16 \text{ m}^3/\text{g-DW}/\text{d}$ ), assimilation efficiency (0.75),  $\text{NH}_4$  excretion rate ( $0.0642 \text{ mg}/\text{g-DW}/\text{h}$ ), and oxygen respiration rates ( $0.9867 \text{ mg}/\text{g-DW}/\text{h}$ ), are well within the estimated rate ranges for local commercial oyster species (e.g., *Crassostrea angulata* and *Crassostrea hongkongensis*) determined from the field or lab experiments.<sup>38,39,41–44</sup>

In summary, the model can skilfully simulate the characteristic physical-biogeochemical processes and hypoxia off PRE and the key oyster-related process rates, which provides a solid foundation for examining oyster aquaculture impacts on hypoxia and ecosystem dynamics.

**3.2. Nutrient Removal Efficiency under Different Oyster Aquaculture Strategies.** The potential of using oyster aquaculture for eutrophication abatement relies on how efficiently the nutrients are removed by oysters.<sup>22</sup> Below, we focus the nutrient removal on nitrogen only, but the same should hold for phosphorus since our model parametrization assumed a constant N/P ratio following the Redfield stoichiometry. We determine oyster removal of nitrogen as the difference between the nitrogen assimilated and the nitrogen lost. The nitrogen lost is resulted from oyster excretion (which produces  $\text{NH}_4$ ) and mortality (which produces particulate nitrogen that enters the oyster detritus pool).

The amount of oyster assimilated PON varies depending on the farming location, oyster density, and farm areal size (Figure 3a). With the same oyster density and farm size, the assimilated PON is highest in Case M, followed by Case W, and is lowest in Case E (Figure 3a), which is consistent with the higher farming feasibility index for the western (upstream) zone than the eastern (downstream) zone (Figure S1). Cases M and W have farms upstream of the plume path (Figure 1), where the assimilated PON is nearly equally contributed by the riverine  $\text{POM}_{\text{terr}}$  and the autochthonous phytoplankton. In contrast, for Case E, where the farm is downstream, the phytoplankton dominates the oyster assimilated PON, reflecting the gradually declining terrestrial contribution to the total PON downstream along the path of the river plume.<sup>29</sup>

At the same location and farm areal size, the amount of assimilated PON increases as the oyster density increases from 50 to 400 oysters/ $\text{m}^2$  (i.e., Cases Wd50 to Wd400), but the increase slows down when the density exceeds 200 oysters/ $\text{m}^2$  due to a limitation of food resource. With a fixed oyster density, the amount of assimilated PON increases with the increasing farming area from 10 to 200  $\text{km}^2$  (i.e., Cases Wa10 to Wa200) but at a rate smaller than that of the farming area. This suggests that spatially expanding the oyster farm reduces the assimilation potential per unit area as food resource gets depleted under the rising demand of oyster feeding. Case WE has the same farming areal size and density as Case Wa200 but yields higher assimilated PON, indicating that spatially

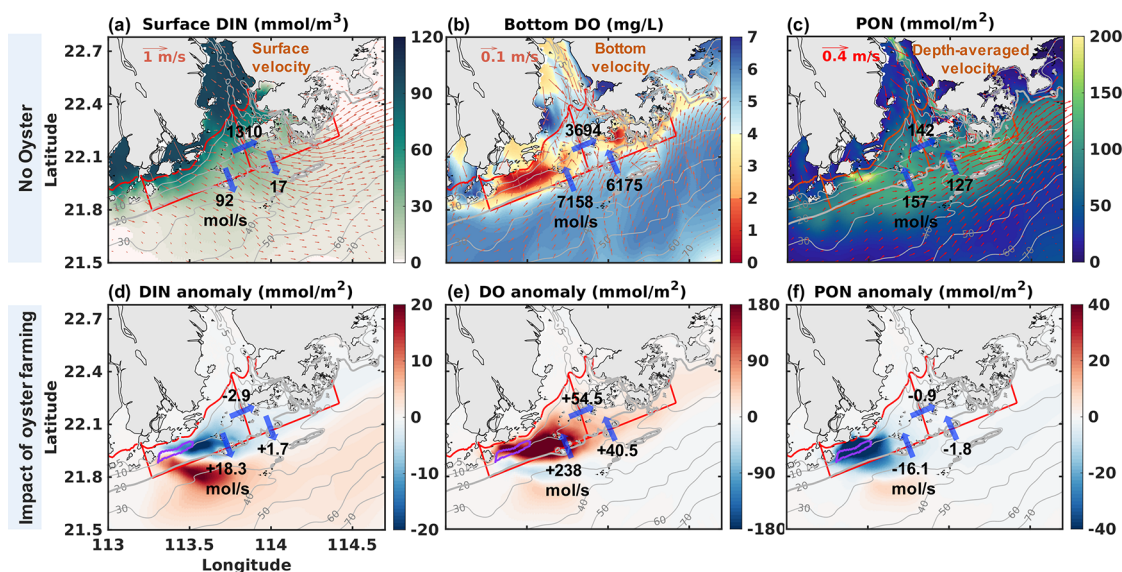


**Figure 4.** Spatial distribution of (a) surface DIN, (b) bottom DO, and (c) water column integrated PON, from the “No\_oyster” case with surface velocity, bottom velocity, and depth-averaged velocity (thin red arrows) superimposed onto the map of each panel, respectively. The solid red lines depict the boundaries of the western and eastern coastal transition zone. The thick blue arrows and accompanying values denote the transect-integrated net transport rates of the respective variable across the corresponding transect. The gray contours mark the bathymetric depths of 5, 10, 20, 30, 40, and 50 m, and a thicker gray 20 m contour line. (d–f) Same as in panels a–c but for the anomaly ( $[\text{Case W} - \text{Case No\_oyster}]$ ) of the water column integrated (d) DIN, (e) DO, and (f) PON. The magenta box denotes the location of the oyster farm in Case W. The values accompanying the thick blue arrows denote the differences in the transect-integrated net transport rates of the respective variable between the W and No\_oyster cases, where the + symbol indicates an increase, and – indicates a decrease of the net transport rate in Case W relative to the No\_oyster case.

dispersing the farms can reduce the feeding pressure among oysters in the immediate surrounding and thus increase the assimilation efficiency of oyster aquaculture.

The amount of  $\text{NH}_4$  excreted by oyster basal metabolism (proportional to the oyster biomass in the farm) and active respiration (proportional to the assimilated PON) also varies under the different farming scenarios (Figure 3b). Since basal metabolism predominantly contributes to the excretion, the differences in the amount of excretion among the different scenarios largely mirror the differences in oyster biomass among the scenarios. Namely, the greater the number of oysters being cultivated, the greater the amount of  $\text{NH}_4$  excreted from the oyster farm. This also holds for oyster mortality, which is parametrized to be proportional to oyster biomass.

Deduction of the amount of excreted  $\text{NH}_4$  and oyster mortality from the assimilated PON (all have units of mol-N) yields the net nitrogen removed by the oysters (solid red dots in Figure 3a). The pattern of net nitrogen removed among different scenarios resembles that of assimilated PON except for the scenarios for which we adjusted the oyster density (i.e., Cases Wd50 to Wd400). In these oyster density scenarios, the removed nitrogen peaks for Wd100 and declines with further increase in density despite the continuously increasing assimilated PON. For the same oyster density and farming location, the nitrogen removal efficiency normalized by farming area (orange dots in Figure 3a) decreases as the farm size grows within a single location (i.e., Cases Wa10 to Wa200) but increases slightly as the farms are dispersed in multiple regions (i.e., higher in Case WE than Wa200).

While the nitrogen removal efficiency reflects the ecological benefit of oyster aquaculture for a eutrophic aquatic system, the biomass accumulation or the net biomass gain of individual oysters (computed as the difference between oyster assim-

ilation and loss terms) during cultivation reflects the economic benefit of growing and harvesting oysters. Figure 3c shows that the net gain of an individual oyster is higher when it is cultivated upstream (Cases W and M) rather than downstream (Case E). The net gain declines as the oyster density or farming areal size increases. The increasing net nitrogen removal (Figure 3a) and decreasing oyster biomass accumulation (Figure 3c) with the increasing number of oysters in a farm (through increasing oyster density and/or expanding the farm) implies a trade-off between the ecosystem and economic benefits of oyster cultivation.

**3.3. Impacts on Biochemical Element Transport and Biogeochemical Processes.** We now assess how oyster aquaculture affects the mass, distribution, and advection of biochemical elements such as dissolved inorganic nitrogen (DIN), dissolved oxygen (DO), and PON, all of which are closely related to oyster filter-feeding and critical to oxygen dynamics.

First, we examine the spatial distributions of DIN, DO, and PON in the No\_oyster case (Figure 4a–c, and see the surface, bottom, and vertically integrated distribution of these variables in SI Figure S2). The surface DIN distribution reflects a seaward spreading nutrient-rich river plume and a wind-driven along-shelf current (Figure 4a). The bottom DO distribution reveals two hypoxic centers in the western and eastern coastal transition zone where the wind-driven shoreward bottom current converges with the buoyant seaward surface flow (Figure 4b). That convergence promotes accumulating PON in the transition zone (Figure 4c). Driven by the eastward wind-driven along-shelf current, the western zone is the net source of DIN, DO, and PON for the eastern zone. The transition zone is a net source of DIN for the outer shelf, because the transition zone receives large amounts of river

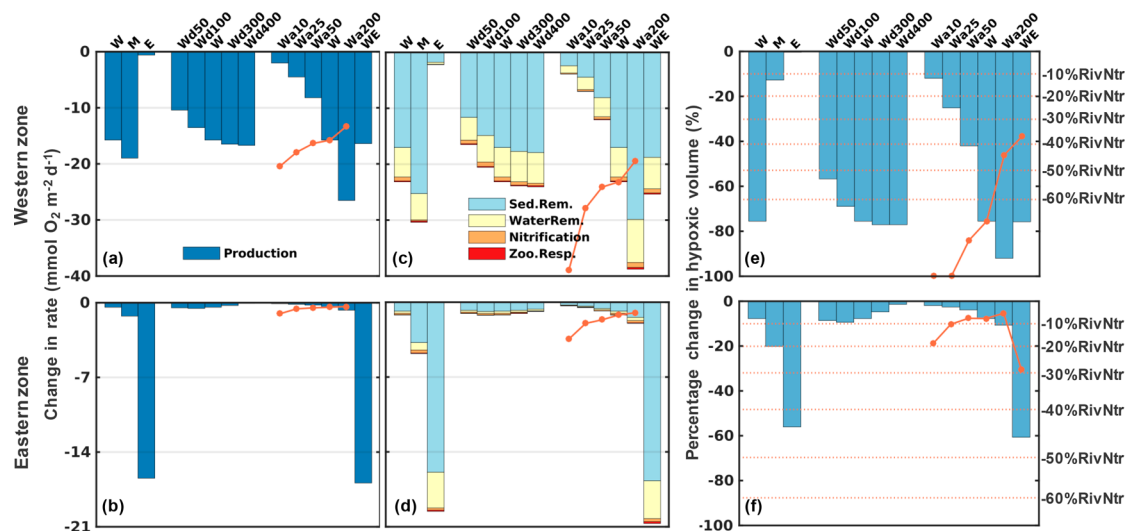


**Figure 5.** Change in the (a, b, c, d) biogeochemical process rates and (e, f) hypoxic volume in the western (upper panels) and eastern (lower panels) coastal transition zone for different farming cases relative to the No\_oyster case. Panels a and b present the change in primary production rate and c and d the change in oxygen-consuming biogeochemical process rates, including sediment remineralization (Sed.Rem.), water column remineralization (WaterRem), nitrification, and zooplankton respiration (Zoo.Resp.). In panels a–d, the dotted orange lines denote the normalized change in primary production rate or total oxygen-consuming process rate per 100 km<sup>2</sup> of farming area (i.e., change/[farming area/100]). All rates were vertically integrated over the water column and spatially averaged over the respective zone. In panels e and f, the horizontal dashed lines denote the percentage change in hypoxic volume by river nutrient reduction cases. The dotted orange lines denote the normalized percentage change in hypoxic volume per 100 km<sup>2</sup> of farming area (i.e., percentage change/[farming area/100]). Values of hypoxic volume (km<sup>3</sup>) and the percentage changes for all scenarios are presented in SI Table S5.

nutrients (Figure 4a), whereas the outer shelf is a net source of DO and PON to the transition zone (Figure 4b,c).

Oyster aquaculture strongly affects the distribution of biochemical elements in the water within and adjacent to oyster farms (Figure 4d–f). Expectedly, there is a substantial drop in PON (Figure 4f) and an increase in DO (Figure 4e) surrounding the oyster farm. The change in DIN due to oyster farming has two opposing modes (Figure 4d): an onshore decrease in DIN that could be attributed to the reduced PON remineralization following oyster filtration, and an offshore increase in DIN due to oyster excretion of NH<sub>4</sub>. The farming-induced change in the spatial distribution of the biochemical elements further affects their along-shore and cross-shore transports (thick arrows in Figure 4d–f). In the along-shore direction, the oyster farming in the western zone reduces the eastward transport of DIN and PON while increasing the DO transport, all of which favor hypoxia reduction in the eastern zone. In the cross-shore direction, the oyster farming in the western zone enhances the offshore DIN transport and shoreward DO transport while reducing the shoreward PON transport, which helps alleviate hypoxia in the entire transition zone (Figure 4d–f). When the oyster density or farm size upstream increases (Cases Wd50 to Wd400 and Wa10 to Wa200), the excreted DIN increases, which further enhances the offshore DIN transport across the western section of the along-shore transect while reducing that across the eastern section (SI Figure S3). This reveals that nutrient effluents from extremely intensive oyster farming upstream can reduce downstream benefits regarding eutrophication mitigation. Nevertheless, the overall impact of these offshore advected nutrient effluents on the ecosystem will be weak as they are advected away from the coastal transition zone that is susceptible to hypoxia.

Next, we assess how different oyster aquaculture scenarios affect the primary production and oxygen-consuming bio-

geochemical processes in the coastal transition zone (Figure 5). Here, the rates are presented in terms of oxygen, but they can be proportionally converted to nitrogen based on the constant Redfield stoichiometric ratios adopted in the model. In the western (upstream) zone, a substantial decrease in primary production is observed in all scenarios with oyster farms in the west (Figure 5a), and the pattern largely mirrors that of the assimilated PON (Figure 3a) because phytoplankton is the major food source for oysters. Reduced primary production means reduced autochthonous organic matter, which, with the filtration-reduced POM<sub>terr</sub> (Figure 3a), lead to substantially reduced sediment and water column OM remineralization rates (Figure 5c). It is worth noting that while Case M has a larger reduction in oxygen-consuming process rates than Case W when averaged over the western zone (Figure 5c), the result is opposite when averaged over the low-oxygen (DO < 3 mg/L) region (Figure S4b). Increasing the oyster density (i.e., Wd50 to Wd400) or expanding the farm size (i.e., Wa10 to Wa200) generally enhances the reductions in primary production (Figure 5a) and oxygen-consuming process rates (Figure 5c), yet the enhancement weakens with the increasing oyster density and the reduction per 100 km<sup>2</sup> declines with increasing farm size (Figure 5a,c). Such pattern is consistent with the pattern observed in the assimilated PON (Figure 3a).

In the eastern (downstream) zone, the reductions in primary production (Figure 5b) and oxygen-consuming process rates (Figure 5d) are small for all scenarios except for Cases E and WE that have an oyster farm in the eastern zone. This further confirms that the direct changes in filtration-induced biogeochemical processes are most pronounced within or adjacent to the oyster farms and are relatively minor downstream. Nevertheless, increasing the oyster cultivation density or farm size upstream does affect the downstream processes in the eastern zone. For the eastern (downstream)

zone, the reduction of oxygen-consuming process rates peaks in Case Wd100 and then decreases as the oyster density increases (Wd200 to Wd400) (Figure 5d), and the reduction normalized by farm area decreases as the farm size expands upstream (Wa10 to Wa200). We attribute such responses to the increased  $\text{NH}_4$  excretion from the oysters with increasing oyster density or farming area upstream (Figure S3) as we earlier discussed.

**3.4. Optimal Oyster Aquaculture Strategies for Reducing Hypoxia.** In this section, we examine the impact of different oyster aquaculture strategies on hypoxia reduction (relative to the No\_oyster case) (Figure 5e,f and SI Table S5). We find that deploying the farm in the upper water layer above the bottom hypoxic zone maximizes hypoxia reduction; for example, hypoxia reduction in the western coastal transition zone is significantly larger in Case W (76% reduction in hypoxic volume) than in Case M (13%) (Figure 5e). This larger hypoxia reduction is due to the larger reduction in oxygen consumption, especially from sediment, in the low-oxygen zone in Case W (SI Figure S4b). Cultivating oysters in the western (upstream) zone alleviates hypoxia in the eastern (downstream) zone (e.g., reduced by 8% in Case W and 20% in Case M), but the reduction is relatively small compared to the reduction by oyster farming in the eastern zone (56% in Case E and 61% in Case WE) (Figure 5f). When oysters are farmed in the western zone, increasing the cultivation density or expanding farming areal size leads to larger hypoxia reduction in the western zone, but the reduction saturates or slows down when the density or areal size exceeds a threshold (200 oysters/m<sup>2</sup> and 100 km<sup>2</sup>) (Figure 5e). A similar trend holds for the hypoxia reduction in the eastern zone except that the hypoxia reduction starts to decline once the upstream oyster density exceeds 100 oysters/m<sup>2</sup> (Figure 5f). Furthermore, for both western and eastern zones, hypoxia reduction normalized by farm areal size generally decreases with increasing farm size, suggesting that the effectiveness of hypoxia abatement per unit farming area declines with the farm expansion. This pattern of hypoxia reductions among different model runs (Figure 5e,f) is very similar to the pattern of reductions in total oxygen consumption rate (Figure 5c,d), suggesting that the filtration-induced reduction in oxygen-consuming process rates, dominated by sediment OM remineralization, largely determines the magnitude of hypoxia reduction.

Finally, we compare the effectiveness of hypoxia reduction by oyster aquaculture to hypoxia mitigation by reducing river nutrient inputs (Figure 5e,f, and SI Figure S5 and Table S5). The comparison reveals that an oyster aquaculture area of 10 to 200 km<sup>2</sup> in the western zone reduces hypoxic volume by 10% to 78% in the entire coastal transition zone, which equals or is greater than the hypoxia reduction achieved by reducing 10% to 60% of the river nutrient input (SI Figure S5 and Table S5). However, the hypoxia reduction achieved by oyster farming is mostly limited to either the western or eastern zone where there is an oyster farm, while the reduction achieved by reducing riverine nutrients is spatially more evenly distributed, benefiting both the western and eastern zones (Figure 5e,f).

**3.5. Implications for Eutrophication and Hypoxia Abatement.** By incorporating the oyster filter-feeding processes into a coupled physical-biogeochemical model, this study quantifies how effective oyster aquaculture can remove nutrients and alleviate hypoxia in a dynamic estuarine system, which provides implications for the initiative of expanding

shellfish farming to abate eutrophication in many regions worldwide.<sup>9,24</sup> We show that the hypoxia reduction caused by oyster farming is largely because oyster ingestion on POM reduces sediment OM remineralization, which not only reduces oxygen consumption directly but also reduces the amount of regenerated nutrients that can support the new production of OM. There has been debate on whether the increased biodeposition underneath shellfish farms offsets the benefit of shellfish nutrient removal,<sup>45</sup> especially in locations where current speeds are low and/or there are excessively high shellfish cultivation densities.<sup>23,25</sup> Our experiments reveal that the increase of sediment oxygen consumption derived from oyster deposits is much lower than the reduction of sediment oxygen consumption resulting from the reduced depositing POM flux following oyster filtration (i.e., the former is about 1% of the latter in magnitude). The negligible impact of oyster biodeposition found here is consistent with the field measurements in a fjord in Denmark where mussel farming prevails.<sup>11</sup> It suggests that shellfish biodeposition might not be a concern for an aquatic system that has a relatively strong current such as the wind-driven current off the PRE. Nevertheless, future work is required on the effects of biodeposition from shellfish farms under different hydrodynamic conditions and it may require models with a higher spatial resolution to resolve the effect of oyster farms on the current field.

Implementing oyster farms for eutrophication abatement requires sound planning (e.g., farming location, cultivation density, and farm areal size) to maximize the ecological (via nitrogen removal and hypoxia reduction) and economic (via oyster biomass accumulation or growth) benefits. Our results show that oyster farms located in or close to the upper water of the low-oxygen zone achieve the largest reduction in sediment oxygen consumption within the zone and thus largest hypoxia reduction, and the reduction increases with increasing oyster density and/or expanding farming area until oyster feeding becomes limited by food resources. However, when oysters are farmed upstream of the hypoxic zone, the farming-induced hypoxia reduction is small and generally decreases with the increasing oyster density or farm areal size, because nutrient effluents from the upstream farms can support downstream production of organic matter. Interestingly, when farming in the upper water of the hypoxic zone, increasing oyster density yields larger hypoxia reduction locally but reduces biomass accumulation of individual oysters due to the increasing feeding pressure. This implies a trade-off between hypoxia reduction and oyster growth in altering oyster cultivation density, which has important implications for the deployment and/or expansion of shellfish farms in the PRE and other systems. Some overintensive oyster cultivation in the coastal waters adjacent to the PRE has impaired oyster growth in recent years.<sup>40</sup> The biogeochemical model presented here can serve as a useful tool to optimize oyster farming in achieving maximum ecological and economic benefits.

Finally, we show that an oyster aquaculture area of 10 to 100 km<sup>2</sup> in the western coastal transition zone reduces hypoxic volume by 10% to 64% in the entire transition zone off the PRE, which equals the hypoxia reduction achieved by reducing 10% to 50% of the river nutrient input. A farm size of 200 km<sup>2</sup> distributed in the western and eastern zones reduces the hypoxic volume by 73% in the entire transition zone, which is equivalent to the impact of reducing river nutrient load by 60%. Given the complexity and scale of river nutrient input reduction, especially those contributed by nonpoint nutrient

sources such as agriculture and urban runoff, the substantial reduction in hypoxia off the PRE by oyster aquaculture renders it a promising nutrient management strategy, although future work is required on the feasibility of farm implementation.

In summary, our investigation highlights the potential use of oyster aquaculture to complement land-based measures for mitigating coastal eutrophication and hypoxia. Our results also reveal that the effectiveness of oyster aquaculture on hypoxia reduction depends on the farming location, farm areal size, and oyster density. Optimal operational strategies must take into account the circulation and biogeochemical characteristics of the specific aquatic system.

## ■ ASSOCIATED CONTENT

### SI Supporting Information

The Supporting Information is available free of charge at <https://pubs.acs.org/doi/10.1021/acs.est.0c06616>.

Description of the coupled physical-biogeochemical model; biogeochemical model state variables, equations, and parameter values (PDF)

## ■ AUTHOR INFORMATION

### Corresponding Author

Jianping Gan – Department of Ocean Science and Department of Mathematics, The Hong Kong University of Science and Technology, Hong Kong, China; Phone: (852)2358 7421/2358 8363; Email: [magan@ust.hk](mailto:magan@ust.hk); Fax: (852)2335 9317/2358 1643

### Author

Liuqian Yu – Department of Ocean Science and Department of Mathematics, The Hong Kong University of Science and Technology, Hong Kong, China; [orcid.org/0000-0002-5492-8213](https://orcid.org/0000-0002-5492-8213)

Complete contact information is available at: <https://pubs.acs.org/10.1021/acs.est.0c06616>

### Notes

The authors declare no competing financial interest.

## ■ ACKNOWLEDGMENTS

This research was supported by the Theme-based Research Scheme (T21-602/16-R, OCEAN\_HK project) of the Hong Kong Research Grants Council. We acknowledge the support of the National Supercomputer Center of Tianhe-1 (Tianjin) and Tianhe-2 (Guangzhou). The ROMS code to generate the model output is available at <https://www.myroms.org/>. The observational data used in this research is available in Supporting Information. We also thank two anonymous reviewers for their constructive reviews.

## ■ REFERENCES

- (1) Diaz, R. J.; Rosenberg, R. Spreading Dead Zones and Consequences for Marine Ecosystems. *Science* **2008**, *321* (5891), 926–929.
- (2) Breitburg, D.; Levin, L. A.; Oschlies, A.; Grégoire, M.; Chavez, F. P.; Conley, D. J.; Garçon, V.; Gilbert, D.; Gutiérrez, D.; Isensee, K.; Jacinto, G. S.; Limburg, K. E.; Montes, I.; Naqvi, S. W. A.; Pitcher, G. C.; Rabalais, N. N.; Roman, M. R.; Rose, K. A.; Seibel, B. A.; Telszewski, M.; Yasuhara, M.; Zhang, J. Declining Oxygen in the Global Ocean and Coastal Waters. *Science* **2018**, *359* (6371), No. 7240.
- (3) Rabalais, N. N.; Cai, W. J.; Carstensen, J.; Conley, D. J.; Fry, B.; Hu, X.; Quiñones-Rivera, Z.; Rosenberg, R.; Slomp, C.; Turner, E.; Voss, M.; Wissel, B.; Zhang, J. Eutrophication-Driven Deoxygenation in the Coastal Ocean. *Oceanography* **2014**, *27* (1), 172–183.
- (4) Duarte, C. M.; Krause-Jensen, D. Intervention Options to Accelerate Ecosystem Recovery From Coastal Eutrophication. *Frontiers in Marine Science* **2018**, *5* (470), 1–8.
- (5) Boesch, D. F. Barriers and Bridges in Abating Coastal Eutrophication. *Frontiers in Marine Science* **2019**, *6* (123), 1–25.
- (6) Funkey, C. P.; Conley, D. J.; Reuss, N. S.; Humborg, C.; Jilbert, T.; Slomp, C. P. Hypoxia Sustains Cyanobacteria Blooms in the Baltic Sea. *Environ. Sci. Technol.* **2014**, *48* (5), 2598–2602.
- (7) Conley, D. J.; Carstensen, J.; Aigars, J.; Axe, P.; Bonsdorff, E.; Eremina, T.; Hahti, B.-M.; Humborg, C.; Jonsson, P.; Kotta, J.; Lännegren, C.; Larsson, U.; Maximov, A.; Medina, M. R.; Lysiak-Pastuszak, E.; Remeikaitė-Nikiėnė, N.; Walve, J.; Wilhelms, S.; Zillén, L. Hypoxia Is Increasing in the Coastal Zone of the Baltic Sea. *Environ. Sci. Technol.* **2011**, *45* (16), 6777–6783.
- (8) Carmichael, R. H.; Walton, W.; Clark, H. Bivalve-Enhanced Nitrogen Removal from Coastal Estuaries. *Can. J. Fish. Aquat. Sci.* **2012**, *69* (7), 1131–1149.
- (9) Rose, J. M.; Bricker, S. B.; Tedesco, M. A.; Wikfors, G. H. A Role for Shellfish Aquaculture in Coastal Nitrogen Management. *Environ. Sci. Technol.* **2014**, *48* (5), 2519–2525.
- (10) Bricker, S. B.; Ferreira, J. G.; Zhu, C.; Rose, J. M.; Galimany, E.; Wikfors, G. H.; Saurer, C.; Miller, R. L.; Wands, J.; Trowbridge, P.; Grizzle, R.; Wellman, K.; Rheault, R.; Steinberg, J.; Jacob, A.; Davenport, E. D.; Ayvazian, S.; Chintala, M.; Tedesco, M. A. Role of Shellfish Aquaculture in the Reduction of Eutrophication in an Urban Estuary. *Environ. Sci. Technol.* **2018**, *52*, 173–183.
- (11) Petersen, J. K.; Timmermann, K.; Carlsson, M.; Holmer, M.; Maar, M.; Lindahl, O. Mussel Farming Can Be Used as a Mitigation Tool - A Reply. *Mar. Pollut. Bull.* **2012**, *64* (2), 452–454.
- (12) Petersen, J. K.; Hasler, B.; Timmermann, K.; Nielsen, P.; Tørring, D. B.; Larsen, M. M.; Holmer, M. Mussels as a Tool for Mitigation of Nutrients in the Marine Environment. *Mar. Pollut. Bull.* **2014**, *82* (1–2), 137–143.
- (13) Cerco, C. F.; Noel, M. R. Can Oyster Restoration Reverse Cultural Eutrophication in Chesapeake Bay? *Estuaries Coasts* **2007**, *30* (2), 331–343.
- (14) Kellogg, M. L.; Smyth, A. R.; Luckenbach, M. W.; Carmichael, R. H.; Brown, B. L.; Cornwell, J. C.; Piehler, M. F.; Owens, M. S.; Dalrymple, D. J.; Higgins, C. B. Use of Oysters to Mitigate Eutrophication in Coastal Waters. *Estuarine, Coastal Shelf Sci.* **2014**, *151* (C), 156–168.
- (15) Bricker, S. B.; Grizzle, R. E.; Trowbridge, P.; Rose, J. M.; Ferreira, J. G.; Wellman, K.; Zhu, C.; Galimany, E.; Wikfors, G. H.; Saurer, C.; Miller, R. L.; Wands, J.; Rheault, R.; Steinberg, J.; Jacob, A. P.; Davenport, E. D.; Ayvazian, S.; Chintala, M.; Tedesco, M. A. Bioextractive Removal of Nitrogen by Oysters in Great Bay Piscataqua River Estuary, New Hampshire, USA. *Estuaries Coasts* **2020**, *43*, 23–38.
- (16) Ferreira, J. G.; Hawkins, A. J. S.; Bricker, S. B. Management of Productivity, Environmental Effects and Profitability of Shellfish Aquaculture — the Farm Aquaculture Resource Management (FARM) Model. *Aquaculture* **2007**, *264* (1–4), 160–174.
- (17) Conley, D. J.; Humborg, C.; Rahm, L.; Savchuk, O. P.; Wulff, F. Hypoxia in the Baltic Sea and Basin-Scale Changes in Phosphorus Biogeochemistry. *Environ. Sci. Technol.* **2002**, *36*, 5315–5320.
- (18) Conley, D. J.; Björck, S.; Bonsdorff, E.; Carstensen, J.; Destouni, G.; Gustafsson, B. G.; Hietanen, S.; Kortekaas, M.; Kuosa, H.; Meier, H. E. M.; Müller-Karulis, B.; Nordberg, K.; Norkko, A.; Nürnberg, G.; Pitkänen, H.; Rabalais, N. N.; Rosenberg, R.; Savchuk, O. P.; Slomp, C. P.; Voss, M.; Wulff, F.; Zillén, L. Hypoxia-Related Processes in the Baltic Sea. *Environ. Sci. Technol.* **2009**, *43* (10), 3412–3420.
- (19) Petersen, J. K.; Saurer, C.; Nielsen, P.; Timmermann, K. The Use of Shellfish for Eutrophication Control. *Aquacult. Int.* **2016**, *24* (3), 857–878.

- (20) Forrest, B. M.; Keeley, N. B.; Hopkins, G. A.; Webb, S. C.; Clement, D. M. Bivalve Aquaculture in Estuaries: Review and Synthesis of Oyster Cultivation Effects. *Aquaculture* **2009**, *298* (1–2), 1–15.
- (21) Stephenson, K.; Aultman, S.; Metcalfe, T.; Miller, A. An Evaluation of Nutrient Nonpoint Offset Trading in Virginia: A Role for Agricultural Nonpoint Sources? *Water Resour. Res.* **2010**, *46* (4), 29–11.
- (22) Rose, J. M.; Bricker, S. B.; Ferreira, J. G. Comparative Analysis of Modeled Nitrogen Removal by Shellfish Farms. *Mar. Pollut. Bull.* **2015**, *91* (1), 185–190.
- (23) Lindahl, O.; Hart, R.; Hernroth, B.; Kollberg, S.; Loo, L.-O.; Olog, L.; Rehnstam-Holm, A.-S.; Svensson, J.; Svensson, S.; Syversen, U. Improving Marine Water Quality by Mussel Farming: A Profitable Solution for Swedish Society. *Ambio* **2005**, *34* (2), 131.
- (24) Kotta, J.; Futter, M.; Kaasik, A.; Liversage, K.; Ratsep, M.; Barboza, F. R.; Bergstrom, L.; Bergstrom, P.; Bobsien, I.; Diaz, E.; Herkul, K.; Jonsson, P. R.; Korpinen, S.; Kraufvelin, P.; Krost, P.; Lindahl, O.; Lindegarth, M.; Lyngsgaard, M. M.; Muhl, M.; Sandman, A. N.; Orav-Kotta, H.; Orlova, M.; Skov, H.; Rissanen, J.; Sialyus, A.; Vidakovic, A.; Virtanen, E. Cleaning up Seas Using Blue Growth Initiatives: Mussel Farming for Eutrophication Control in the Baltic Sea. *Sci. Total Environ.* **2020**, *709* (C), 136144.
- (25) Higgins, C. B.; Stephenson, K.; Brown, B. L. Nutrient Bioassimilation Capacity of Aquacultured Oysters: Quantification of an Ecosystem Service. *Journal of Environmental Quality* **2011**, *40* (1), 271–277.
- (26) Humphries, A. T.; Ayvazian, S. G.; Carey, J. C.; Hancock, B. T.; Grabbert, S.; Cobb, D.; Strobel, C. J.; Fulweiler, R. W. Directly Measured Denitrification Reveals Oyster Aquaculture and Restored Oyster Reefs Remove Nitrogen at Comparable High Rates. *Frontiers in Marine Science* **2016**, *3*, 107–110.
- (27) Zhao, H. *Evolution of the Pearl River Estuary*; China Ocean Press, Beijing, 1990.
- (28) Li, D.; Gan, J.; Hui, R.; Liu, Z.; Yu, L.; Lu, Z.; Dai, M. Vortex and Biogeochemical Dynamics for the Hypoxia Formation within the Coastal Transition Zone off the Pearl River Estuary. *Journal of Geophysical Research O* **2020**, *125* (8), 1–16.
- (29) Yu, L.; Gan, J.; Dai, M.; Hui, C. R.; Lu, Z.; Li, D. Modeling the Role of Riverine Organic Matter in Hypoxia Formation within the Coastal Transition Zone off the Pearl River Estuary. *Limnology and Oceanography* **2020**, *9999* (2020), 1–17.
- (30) *China Fishery Statistical Yearbook*; Bureau of Fisheries of Ministry of Agriculture, 2019.
- (31) Botta, R.; Asche, F.; Borsum, J. S.; Camp, E. V. A Review of Global Oyster Aquaculture Production and Consumption. *Marine Policy* **2020**, *117*, 103952.
- (32) Shchepetkin, A. F.; McWilliams, J. C. The Regional Oceanic Modeling System (ROMS): A Split-Explicit, Free-Surface, Topography-Following-Coordinate Oceanic Model. *Ocean Model* **2005**, *9* (4), 347–404.
- (33) Liu, Z.; Gan, J. A Modeling Study of Estuarine-Shelf Circulation Using a Composite Tidal and Subtidal Open Boundary Condition. *Ocean Modelling* **2020**, *147*, 101563.
- (34) Fennel, K.; Wilkin, J.; Levin, J.; Moisan, J.; O'Reilly, J.; Haidvogel, D. Nitrogen Cycling in the Middle Atlantic Bight: Results from a Three-Dimensional Model and Implications for the North Atlantic Nitrogen Budget. **2006**, *20* (3), 2456 DOI: 10.1029/2005gb002456.
- (35) Fennel, K.; Hu, J.; Laurent, A.; Marta-Almeida, M.; Hetland, R. Sensitivity of Hypoxia Predictions for the Northern Gulf of Mexico to Sediment Oxygen Consumption and Model Nesting. *Journal of Geophysical Research: Oceans* **2013**, *118* (2), 990–1002.
- (36) Gan, J.; Lu, Z.; Cheung, A.; Dai, M.; Liang, L.; Harrison, P. J.; Zhao, X. Assessing Ecosystem Response to Phosphorus and Nitrogen Limitation in the Pearl River Plume Using the Regional Ocean Modeling System (ROMS). *Journal of Geophysical Research: Oceans* **2014**, *119* (12), 8858–8877.
- (37) Cerco, C. F.; Noel, M. R. Assessing a Ten-Fold Increase in the Chesapeake Bay Native Oyster Population. **2005**, 1–82.
- (38) Yu, Z.; Zhou, Y.; Qi, Z.; Luo, P.; Hu, C. Temporal Dynamics in Clearance Rate of the Portuguese Oyster *Crassostrea Angulata* Cultivated in Dapeng Cove, Southern China. *Aquaculture* **2017**, *479*, 824–828.
- (39) Lin, L.; Liao, W.; Xie, J.; Zhu, C.; Zhang, H. Effect of Salinity on the Feeding and Metabolic Physiology of *Crassostrea Hongkongensis*. *Guangdong Agricultural Sciences* **2012**, *11*, 10–14.
- (40) Yu, Z.; Jiang, T.; Xia, J.; Ma, Y.; Zhang, T. Ecosystem Service Value Assessment for an Oyster Farm in Dapeng Cove. *Journal of Fisheries of China* **2014**, *38*, 853–860.
- (41) Liao, W.; Zhu, C.; Zhang, H. Effect of Sizes on the Feeding and Metabolic Physiology of *Crassostrea Hongkongensis*. *Chinese Fishery Quality and Standards* **2011**, *1* (3), 41–46.
- (42) Liao, W.; Zhu, C.; Zhang, H.; Wu, J.; Huang, H.; Zhu, F.; Su, L. Effect of Water Temperature on the Feeding and Metabolic Physiology of *Crassostrea Hongkongensis*. *Guangdong Agricultural Sciences* **2011**, *1*, 7–11.
- (43) Wang, G.; Zhang, Q.; Yu, Z.; Lin, X. Effect of Salinity on Oxygen Consumption, Ammonia-N Excretion Rate, O:N and Absorption Efficiency of *Crassostrea Hongkongensis*. *Marine Sciences* **2013**, *37* (2), 101–106.
- (44) Yin, L.; Gao, Y.; Yang, Z.; Yu, Z. Effects of Body Size on Respiration and Excretion of Hong Kong Oyster *Crassostrea Hongkongensis*. *Journal of Tropical Oceanography* **2013**, *32* (1), 60–63.
- (45) Stadmark, J.; Conley, D. J. Mussel Farming as a Nutrient Reduction Measure in the Baltic Sea: Consideration of Nutrient Biogeochemical Cycles. *Mar. Pollut. Bull.* **2011**, *62* (7), 1385–1388.